THE JOURNAL OF PHYSICAL CHEMISTRY B

Article

pubs.acs.org/JPCB

Osmotic Virial Coefficients of Hydroxyethyl Starch from Aqueous Hydroxyethyl Starch−Sodium Chloride Vapor Pressure Osmometry

Jingjiang Cheng,[†] Martin Gier,[‡] Lisa U. Ross-Rodriguez,[†,§] Vinay Prasad,[†] Janet A. W. Elliott,*[,†,§] and Andreas Sputtek[∥]

[†]Department of Chemical and Materials Engineering, University of Alberta, Canada

[‡]Swisslab GmbH, Berlin, Germany

[§]Department of Laboratory Medicine and Pathology, University of Alberta, Canada

[∥]MVZ Labor Limbach Neumünster, Neumünster, Germany

Supporting Information

ABSTRACT: Hydroxyethyl starch (HES) is an important industrial additive in the paper, textile, food, and cosmetic industries and has been shown to be an effective cryoprotectant for red blood cells; however, little is known about its thermodynamic solution properties. In many applications, in particular those in biology, HES is used in an aqueous solution with sodium chloride (NaCl). The osmotic virial solution thermodynamics approach accurately captures the dependence of osmolality on molality for many types of solutes in aqueous systems, including electrolytes, sugars, alcohols, proteins, and starches. Elliott et al. proposed mixing rules for the osmotic virial equation to be used for osmolality of multisolute aqueous solutions [Elliott, J. A. W.; et al. *J. Phys. Chem. B* **2007**, *111*, 1775−1785] and recently applied this approach to the fitting of one set of aqueous HES−NaCl solution data reported by Jochem and Körber [*Cryobiology* **1987**, *24*, 513−536], indicating that the HES osmotic virial coefficients are dependent on HES-to-NaCl mass ratios. The current study reports new aqueous HES−NaCl vapor pressure osmometry data which are analyzed using the osmotic virial equation. HES modifications were measured after dialysis (membrane cut off: 10 000 g/mol) and freeze-drying using vapor pressure osmometry at different mass ratios of HES to NaCl for HES up to 50% and NaCl up to 25% with three different HES modifications (weight average molecular weights [g/mol]/degree of substitution: 40 000/0.5; 200 000/0.5; 450 000/0.7). Equations were then fit to the data to provide a model for HES osmotic virial coefficient dependence on mass ratio of HES to NaCl. The osmolality data of the three HES modifications were accurately described over a broad range of HES-to-NaCl mass ratios using only four parameters, illustrating the power of the osmotic virial approach in analyzing complex data sets. As expected, the second osmotic virial coefficients increase with molecular weight of the HES and increase with HES-to-NaCl mass ratio.

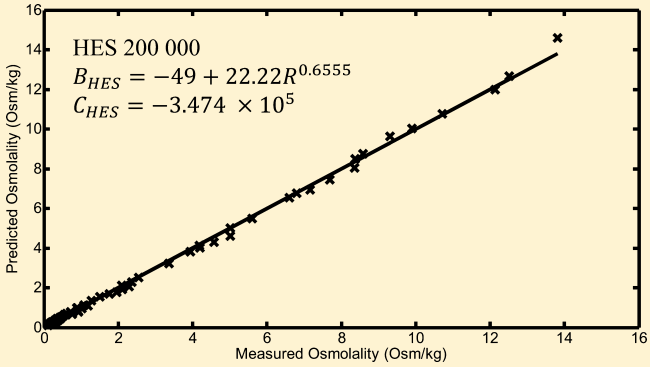

INTRODUCTION

Cryopreservation is the only method routinely used for the long-term preservation of cells and tissues for transfusion, transplantation, and research. Traditional preservation protocols require the addition of cryoprotectants to mitigate cellular injury because of ice formation. The methods for the cryopreservation of red blood cells primarily utilize glycerol and require deglycerolization post-thaw, which is time-consuming and expensive. Inadequate deglycerolization may result in hemolytic transfusion reactions and renal failure. Cryopreservation of red blood cells is advantageous for patients with rare blood groups or adverse antibody problems, for autologous use, and for military disaster relief applications.[1] It can also be used in diagnostics for blood typing, antibody screening, and compatibility testing. Hydroxyethyl starch (HES) has been shown to be an effective cryoprotectant for red blood cells[2−4] and does not require removal prior to transfusion provided the maximum dosage (2 to 3 g/kg of bodyweight) is not exceeded, thus eliminating post-thaw manipulation of the cells and undesirable side effects in the recipients. However, in the case that it needs to be removed, this can be done in a simple centrifugation step because HES does not enter into the cells. In addition to its use in cryopreservation protocols, HES is the main component in plasma expanders such as Pentaspan, used to treat hypotensive and hypovolemic patients by direct infusion. HES thus would be an ideal cryoprotectant in various blood products and emerging cellular therapies that could be infused directly into

Received: April 5, 2013
Revised: July 12, 2013
Published: July 17, 2013

the recipients after cryopreservation without further manipulation. In these biological applications, HES is used in aqueous solution with sodium chloride (NaCl).

Hydroxyalkyl (mostly hydroxyethyl and hydroxypropyl) starches are also used industrially in mass quantities for surface improvement, as additives to dyes used in the textile industry, as glue in both the paper and textile industries, as a clothing starch, and in the food and cosmetic industries.

HES is a modified natural polymer of branched amylopectin (one of the two components of starch; the other component is the linear amylose). Its physical and chemical characteristics are mainly defined by (i) the degree of hydroxyethylation (or degree of substitution, DS), i.e., replacement of hydroxyl groups of the anhydroglucose units by hydroxyethyl groups, and (ii) the molecular weight distribution.[2] Whereas native starch is only slightly water-soluble, hydroxyethylation increases water solubility. DS is determined by measuring the number of substituted anhydroglucose units and dividing this number by the total number of anhydroglucose units in the molecule. The molar substitution (MS) is calculated by measuring the total number of hydroxyethyl groups present and dividing this by the total number of anhydroglucose units. DS and MS are not the same, but they are often incorrectly used interchangeably, especially in the medical literature. As hydroxyethylation can occur at carbon positions 2, 3, or 6 of the anhydroglucose unit, depending on the manufacturing process, the substitution pattern can vary greatly. HES molecules show a great polydispersity, in contrast to most other cryoprotectants, such as the above-mentioned glycerol. The molecular sizes of HES usually follow a bell-shaped distribution, ranging from 1 000 g/mol up to 1 000 000 g/mol, depending on the modification. Consequently, the "molecular weight" reported is usually an average molecular weight. There are two ways to calculate such a molecular weight: (i) arithmetic mean, i.e., total weight of all molecules divided by the number of molecules (M_n), and (ii) the weight averaged mean[2] (M_w), where the contribution of each molecule is weighted by its molecular weight before calculating the mean.

It has been shown in the case of cryopreserved platelets and red blood cells that different modifications of HES produce different cryoprotective effects;[3] thus, it is desirable to gain detailed knowledge of the solution thermodynamics of different HES modifications. Solution thermodynamics refers to obtaining an equation relating the chemical potentials of the components of the solution to temperature, pressure, and composition, but we are in practice most interested in the composition dependence of the water chemical potential, which is given by osmolality as a function of HES concentration.

Specifying osmolality as a function of concentration of multisolute solutions is necessary for modeling low-temperature cellular responses and is also an important consideration for water balance after direct infusion of any product. In the osmotic virial equation,[5] osmolalities are represented as polynomials in concentration with solute-specific osmotic virial coefficients which have been determined for many single solutes in water.[6−14] The multisolute osmotic virial equation has been widely used in many forms[9,13−34] and has been shown to apply for a broad range of low-molecular-weight solutes, including electrolytes, alcohols, and sugars, as well as for high-molecular-weight compounds such as proteins and starches.

Elliott and co-workers[14,33] proposed a form of the multisolute osmotic virial equation that requires only single-solute information to predict multisolute osmolalities. The equation is slightly modified for use with electrolytes by including only one additional single-solute fitting parameter.[34] We have shown that this equation accurately predicts multisolute osmolalities of aqueous solutions containing (i) glycerol and dimethyl sulfoxide,[14,33] (ii) dimethyl sulfoxide and sodium chloride (NaCl),[34] and (iii) ovalbumin and bovine serum albumin.[33] We have also shown that this equation is able to predict the osmolality of the cytoplasmic solution of red blood cells (mainly containing the macromolecule hemoglobin and electrolytes) in agreement with measurements.[24] Other research groups have applied the form of the multisolute osmotic virial equation proposed by Elliott et al. to (i) aqueous solutions of ethylene glycol and sodium chloride,[29] (ii) the quaternary system water−ethylene glycol−sucrose−sodium chloride,[30] and (iii) aqueous solutions of two micelle-forming nonionic surfactants.[31] Recently, Prickett et al.[34] demonstrated the use of the multisolute osmotic virial equation proposed by Elliott et al. to describe the changing macromolecular solution behavior of HES in NaCl aqueous solutions by fitting the equation to the differential scanning calorimetry (DSC) data set published by Jochem and Körber.[35] In that study, the osmotic virial coefficients of HES were described as functions of the HES-to-NaCl mass ratio with seven fit parameters.

Herein, we report a more extensive data set for the osmolalities of three different HES components in aqueous NaCl solutions at different HES-to-NaCl mass ratios measured using vapor pressure osmometry. The multisolute osmotic virial equation proposed by Elliott and co-workers[14,33,34] is fit to the data, yielding simple equations (four fit parameters only) that express the dependence of the HES osmotic virial coefficients on HES-to-NaCl mass ratio and accurately represent the entire data set.

MATERIALS AND EXPERIMENTAL METHODS

Preparation of the Ternary HES−NaCl−Water Solutions. Three high-molecular-weight HES modifications were used in this study: HES 40 000 (lot 58164540, B. Braun Melsungen, Melsungen, Germany), HES 200 000 (lot 901 AH 22, Leopold Pharma, Graz, Austria), and HES 450 000 (lot 1104221, Fresenius, Bad Homburg v.d.H., Germany). Different HES modifications (and even lots with the same modification from the same manufacturer) may contain different amounts of low-molecular-weight impurities, such as electrolytes, sugars, and oligosaccharides. These may have a strong influence on the osmotic properties, especially at the high concentrations used in some experiments in this study. Therefore, the starches were dialyzed at a concentration of approximately 10% by weight with a membrane cutoff of 10 000 to 14 000 g/mol (Serva, Mannheim, Germany, product code 250-7U or 250-9U) against running demineralized water for approximately 2 days. The dialyzed solutions were then concentrated using a rotating evaporator at 60 °C and subsequently freeze-dried within 2 to 3 days in Petri dishes at a pressure below 10^{-2} mbar and a temperature of −50 °C. To further reduce the residual moisture (approximately 5 to 10%), the starches were thereafter stored for approximately 1 week in a desiccator over diphosphorus pentoxide (P_2O_5). The residual moisture content (which was taken into account when preparing the ternary solutions from the starches dried in the desiccator) was determined by drying the starches for another 24 h at approximately 120 °C. The determined moisture contents were 4.8% (HES 200 000), 1.6% (HES 450 000), and 0.2% (HES 40 000). The final molecular

dx.doi.org/10.1021/jp403377b | J. Phys. Chem. B 2013, 117, 10231−10240

weights (shown in Table 1) were determined using a gel permeation chromatography method.

Table 1. HES Molecular Weights

	M_w (g/mol)	M_n (g/mol)
HES 40 000	70 957	42 410
HES 200 000	224 260	64 263
HES 450 000	571 611	116 375

The NaCl (product code 106404) was obtained from Merck (Darmstadt, Germany). Residual moisture was removed by drying the salt at 500 °C for 2 to 3 h followed by cooling in a desiccator. The purity of the water (Delta Pharma, Pfullingen, Germany) corresponded to that of doubly distilled water. After the preparation of all ternary solutions, they were stored frozen at −25 °C until use.

Vapor Pressure Osmometry. Vapor pressure osmometry relies on the principle that the vapor pressure of a solution is different from that of the pure solvent at the same temperature and pressure. Vapor pressure osmometry was conducted at different mass ratios of HES to NaCl, for HES up to 50% and NaCl up to 25% of the solution by mass, with three different HES modifications (Table 1) using a vapor pressure osmometer (type 7334100000, Knauer, Berlin, Germany). In order to reduce potential errors, the measurements were performed in order of increasing concentration of the HES−NaCl mixture. Additionally, we optimized the precision of the instrument in the range of 50−5600 mmol/L (the average deviation of our measured values from values reported in the literature was 0.025%) by establishing a calibration curve using 13 different NaCl solutions, instead of using a single solution of only 300 or 400 mmol/L as recommended by the manufacturer. Means of three repeated measurements for each solution are listed in Table 2. Measurements were done at 37 °C.

DATA ANALYSIS METHODS

The experimental data for this study, collected using the methods described in the previous section, consist of osmolality data obtained at different molalities of HES and NaCl (Table 2). In the data analysis, we seek to describe the osmolality in terms of the molalities of HES and NaCl using the multisolute osmotic virial equation;[14] in order to do this, we need to obtain equations that express accurately the dependence of the HES osmotic virial coefficients on the HES-to-NaCl mass ratio.

Osmotic Virial Equation. The osmolality of a solution, π, is defined by its relationship to the chemical potential[14]

$$\mu_1(T, P, N_i) = \mu_1^*(T, P) - \bar{R}TM_1\pi \tag{1}$$

where μ_1 is the chemical potential of the solvent in the solution, μ_1^* the chemical potential of the pure solvent, T the temperature, P the pressure, N_1 the number of moles of solvent in solution, N_i ($i \geq 2$) the number of moles of solute i, $\bar{R}$ the universal gas constant, and M_1 the molecular weight of the solvent. In eq 1, the chemical potential has units of energy per moles of solvent and the osmolality has units of molality, i.e., moles of solute per kg of solvent. Note that the last term in eq 1 arises from entropic contributions of the solute and as such $\bar{R}T$ is understood to have units of energy per moles of solute. Osmolality, π, is related to osmotic pressure, Π, by

$$\Pi = \bar{R}T\rho_1\pi \tag{2}$$

where ρ_1 is the density of water in kilograms per cubic meter.

The osmotic virial equation (truncated to third order) to predict osmolality in a multisolute solution is[5,14,36]

$$\pi = \sum_i m_i + \sum_i \sum_j B_{ij}m_i m_j + \sum_i \sum_j \sum_k C_{ijk}m_i m_j m_k \tag{3}$$

where m_i is the molality of solute and i, B_{ii}, and C_{iii} are pure solute second and third osmotic virial coefficients respectively (usually simply referred to as B_i and C_i), accounting for interaction between two or three identical solute molecules; B_{ij} and C_{ijk} are cross-coefficients accounting for interaction between solutes i and j or between solutes i, j and k. The single-solute coefficients, B_i and C_i, can be found from fitting the single-solute osmotic virial equation (eq 4) to data.

$$\pi = m_i + B_i(m_i)^2 + C_i(m_i)^3 \tag{4}$$

Prickett et al.[34] showed that the osmotic virial approach can be simply applied to electrolyte solutions by adding one additional fitting parameter, k_{diss}

$$\pi = k_{diss}m_i + B_i(k_{diss}m_i)^2 + C_i(k_{diss}m_i)^3 \tag{5}$$

It is important to note that the empirical parameter k_{diss} accounts for nonideal solution behavior resulting from more than one electrolyte effect, meaning that this "dissociation constant" (sometimes referred to as the van't Hoff factor) may not be exactly equal to two for 1:1 electrolytes, even for electrolytes known to completely dissociate. Prickett et al. showed that the empirical osmotic virial relation in eq 5 described NaCl solution behavior as well as the Pitzer−Debye−Huckel electrolyte theory (both in single-solute solutions and in multisolute solutions).[34]

Mixing rules proposed by Elliott et al.[14] allow the mixed coefficients B_{ij} and C_{ijk} to be written in terms of the single-solute coefficients only:

$$B_{ij} = \frac{B_i + B_j}{2} \tag{6}$$

$$C_{ijk} = (C_iC_jC_k)^{1/3} \tag{7}$$

The osmotic virial equation for an aqueous solution with a macromolecule (HES) and an electrolyte (NaCl) requires second and third osmotic virial coefficients for the macromolecule and a second virial coefficient and additional dissociation constant for the electrolyte in order to describe the nonideal solution behavior.[34] The osmotic virial equation for a ternary system containing HES and NaCl is[34]

$$\pi = k_{diss}m_2 + m_3 + B_2(k_{diss}m_2)^2 + B_3m_3^2 + (B_2 + B_3)k_{diss}m_2m_3 + C_3m_3^3 \tag{8}$$

where k_{diss} is the dissociation constant for NaCl (taken to be 1.678)[33] and B_2 is the second osmotic virial coefficient for NaCl (taken to be 0.044 m^{-1}).[33] B_3 and C_3 are the osmotic virial coefficients of HES, which must be determined as functions of the HES-to-NaCl mass ratio.

Methodology. In eq 8, the molalities of NaCl and HES (m_2 and m_3) and the osmolality (π) are measured quantities and the values of the parameters k_{diss} and B_2 are taken from the literature; this allows us to rearrange eq 8 to obtain

Table 2. Raw Data

mass fraction			ratio	osmolality (mOsm/kg)		
HES	NaCl	H_2O	R	40 000	200 000	400 000
0.0499	0.0030	0.9471	16.6	104	113	118
0.0499	0.0045	0.9456	11.1	168	167	166
0.0499	0.0060	0.9441	8.3	218	219	207
0.0499	0.0090	0.9411	5.5	330	322	323
0.0499	0.0200	0.9301	2.5	1 217	558	559
0.0499	0.0500	0.9001	1.0	1 877	1 765	1 837
0.0499	0.1000	0.8501	0.5	4 093	3 938	4 011
0.0499	0.1500	0.8001	0.3	6 891	6 605	6 713
0.0499	0.2000	0.7501	0.2	10 280	9 897	9 870
0.0499	0.2500	0.7001	0.2	13 471	13 810	13 837
0.0998	0.0030	0.8972	33.3	108	124	130
0.0998	0.0045	0.8957	22.2	176	182	181
0.0998	0.0060	0.8942	16.6	227	234	233
0.0998	0.0090	0.8912	11.1	349	347	359
0.0998	0.0200	0.8802	5.0	743	758	766
0.0998	0.0500	0.8502	2.0	1 956	1 959	1 964
0.0998	0.1000	0.8002	1.0	4 203	4 202	4 212
0.0998	0.1500	0.7502	0.7	7 159	7 159	7 065
0.0998	0.2000	0.7002	0.5	10 749	10 708	10 571
0.1497	0.0030	0.8473	49.9	136	145	139
0.1497	0.0045	0.8458	33.3	164	217	207
0.1497	0.0060	0.8443	25.0	208	262	268
0.1497	0.0090	0.8413	16.6	354	388	374
0.1497	0.0200	0.8303	7.5	508	740	748
0.1497	0.0500	0.8003	3.0	2 097	2 112	2 094
0.1497	0.1000	0.7503	1.5	4 638	4 568	4 592
0.1497	0.1500	0.7003	1.0	7 535	7 686	7 904
0.1497	0.2000	0.6503	0.7	11 650	94.8	11 072
0.1996	0.0030	0.7974	66.5	178	171	173
0.1996	0.0045	0.7959	44.4	241	251	243
0.1996	0.0060	0.7944	33.3	312	324	300
0.1996	0.0090	0.7914	22.2	423	446	446
0.1996	0.0200	0.7804	10.0	882	918	904
0.1996	0.0500	0.7504	4.0	2 163	2 294	2261
0.1996	0.1000	0.7004	2.0	4 939	5 011	4 897
0.1996	0.1500	0.6504	1.3	8 305	8 357	8 300
0.1996	0.2000	0.6004	1.0	11 863	12 516	12 351
0.2495	0.0030	0.7475	83.2	245	220	278
0.2495	0.0045	0.7460	55.4	328	293	335
0.2495	0.0060	0.7445	41.6	375	340	376
0.2495	0.0090	0.7415	27.7	521	480	509
0.2495	0.0200	0.7305	12.5	1 239	905	942
0.2495	0.0500	0.7005	5.0	2 496	2 372	2 445
0.2495	0.1000	0.6505	2.5	5 538	5 010	5 352
0.2495	0.1500	0.6005	1.7	9 205	8 582	8 953
0.2495	0.2000	0.5505	1.2	12 587		13.59
0.2994	0.0030	0.6976	99.8	322	288	299
0.2994	0.0045	0.6961	66.5	453	348	447
0.2994	0.0060	0.6946	49.9	499	425	500
0.2994	0.0090	0.6916	33.3	652	593	628
0.2994	0.0200	0.6806	15.0	1 209	1 087	1 164
0.2994	0.0500	0.6506	6.0	2 739	2 542	2 639
0.2994	0.1000	0.6006	3.0	5 558	5 607	6 404
0.2994	0.1500	0.5506	2.0	9 526	9 304	9 727
0.2994	0.2000	0.5006	1.5			
0.3992	0.0030	0.5978	133.1	543	519	626
0.3992	0.0045	0.5963	88.7	705	620	555
0.3992	0.0060	0.5948	66.5	733	711	735
0.3992	0.0090	0.5918	44.4	955	883	924

dx.doi.org/10.1021/jp403377b | J. Phys. Chem. B 2013, 117, 10231−10240

Table 2. continued

mass fraction			ratio	osmolality (mOsm/kg)		
HES	NaCl	H_2O	R	40 000	200 000	400 000
0.3992	0.0200	0.5808	20.0	1 676	1 506	1 511
0.3992	0.0500	0.5508	8.0		3 371	3 316
0.3992	0.1000	0.5008	4.0	7 324	6 793	6 990
0.3992	0.1500	0.4508	2.7	12 204	12 140	11 384
0.4990	0.0030	0.4980	166.3	1 035	923	1 041
0.4990	0.0045	0.4965	110.9	1 196	1 017	1 145
0.4990	0.0060	0.4950	83.2	1 313	1 184	1 210
0.4990	0.0090	0.4920	55.4	1 527	1 271	1 291
0.4990	0.0200	0.4810	25.0	2 221	2 088	2 118
0.4990	0.0500	0.4510	10.0	4 737	4 183	4 155
0.4990	0.1000	0.4010	5.0	9 384	8 367	8 784

$$\pi - k_{diss}m_2 - m_3 - B_2(k_{diss}m_2)^2 - B_2k_{diss}m_2m_3 = B_3(k_{diss}m_2m_3 + m_3^2) + C_3m_3^3 \quad (9)$$

Equation 9 has the known quantities on the left-hand side and the unknowns B_3 and C_3 and the quantities that multiply them on the right-hand side. We define the mass ratio of HES to NaCl by the symbol R, which is proportional to m_3/m_2.

Figure 1 provides a flowchart of the methodology used to estimate the dependence of B_3 and C_3 on R. Because we do not have a priori knowledge of the functional form of the dependence of these coefficients on R, in step A we group the experimental data into sets of five data points, ordered in increasing values of R. Equation 9 is linear in B_3 and C_3 and can be used to estimate values of B_3 and C_3 at different values of R. The estimated values can provide us with indications about the structure of the function that must be chosen. The minimum number of data points required to obtain values of B_3 and C_3 in a particular range of values of R is two because there are two unknowns. However, we have chosen to use five data points to obtain values of B_3 and C_3; this was based on a series of trials to estimate the best grouping size that would provide information on the functional form without having noisy estimates. Note that a moving window is chosen for grouping, i.e., the sets are $(R_1, R_2, ..., R_n)$, $(R_2, R_3, ..., R_{n+1})$, ..., $(R_{z-n+1}, ..., R_{z-1}, R_z)$ for a grouping size of n. Other methods of smoothing such as Savitzky–Golay filtering[37] can also be used, but they will also provide the same indications on the functional dependence.

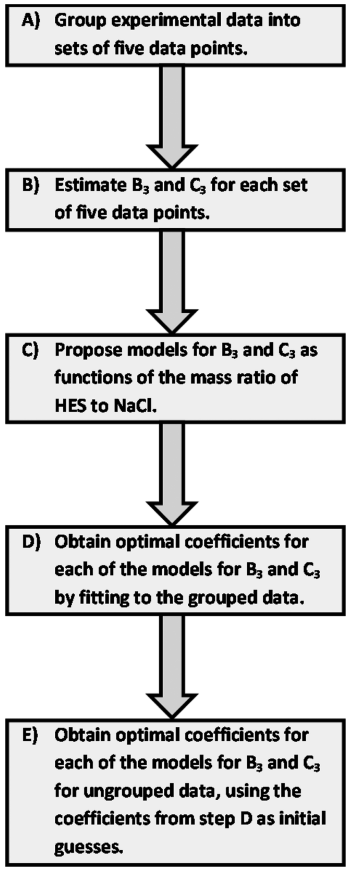

Figure 1. Flowchart of the approach to data analysis.

In step B, we estimate the values of B_3 and C_3 for each set of data points. Equation 9 is of the form

$$Y = X\beta + \varepsilon \quad (10)$$

with Y, X, and β defined as

$$Y = [\pi - k_{diss}m_2 - m_3 - B_2(k_{diss}m_2)^2 - B_2k_{diss}m_2m_3]$$

$$X = [k_{diss}m_2m_3 + m_3^2 \quad m_3^3]$$

$$\beta = \begin{bmatrix} B_3^{est} \\ C_3^{est} \end{bmatrix}$$

ε is the error between the measured and predicted values of Y.

Using standard least-squares estimation, β can be calculated using the following equation (estimated values of variables are denoted by ^):

$$\hat{\beta} = (X^TX)^{-1}X^TY \quad (11)$$

The error between the measured and predicted values of Y is given by

$$\varepsilon = Y - \hat{Y} = Y - X\hat{\beta} \quad (12)$$

and the sum of squared errors, SS_E, by

$$SS_E = \sum \varepsilon^2 \quad (13)$$

The SS_E is the criterion used to judge the accuracy of the fit. The variance of the estimated parameters can be calculated from the diagonal elements of the covariance matrix. The covariance matrix is given by

dx.doi.org/10.1021/jp403377b | J. Phys. Chem. B 2013, 117, 10231−10240

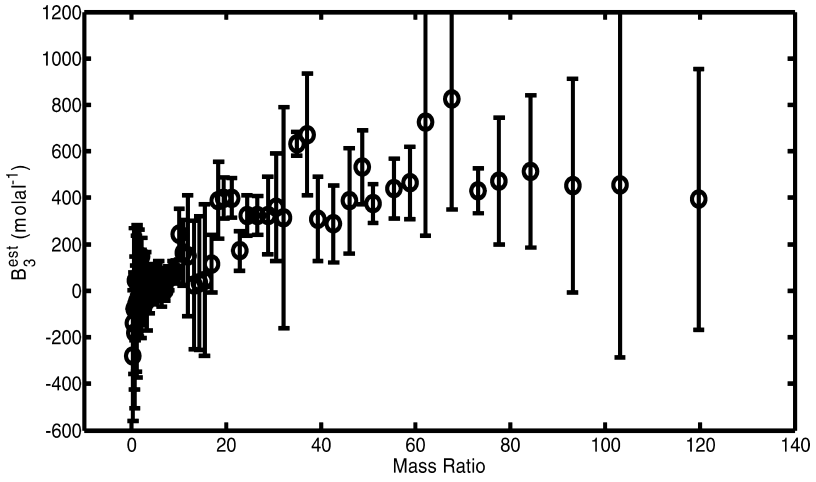

Figure 2. Estimated B_3 values with 95% confidence interval as a function of the mass ratio of HES to NaCl (R) based on grouped data (sets of five data points) for HES 200 000.

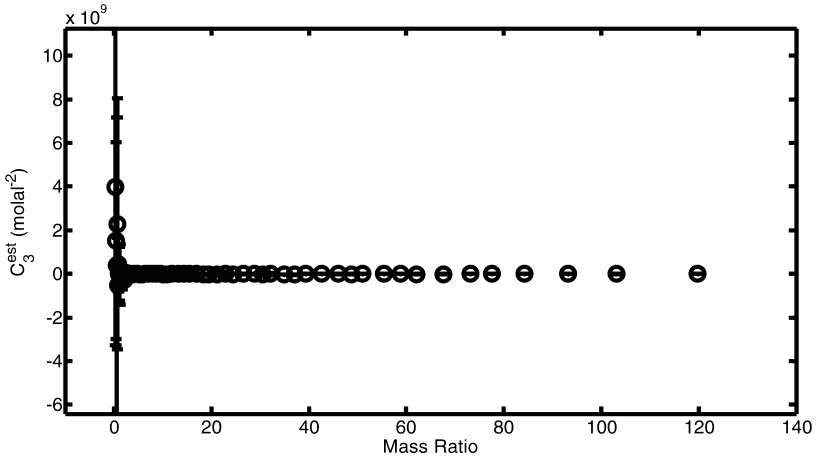

Figure 3. Estimated C_3 values with 95% confidence interval as a function of the mass ratio of HES to NaCl (R) based on grouped data (sets of five data points) for HES 200 000.

Table 3. Models Proposed Based on Estimated Osmotic Virial Coefficients

model	1	2	3	4	5	6	7	8	9
B_3	0	a	a	$a + bR$	$a + bR$	$a + bR^c$	$a + bR^c$	$-a[\exp(-R/b)] - c$	$-a[\exp(-R/b)] - c$
C_3	0	0	d	0	d	0	d	0	d

$$\mathrm{Cov}(\beta) = \hat{\lambda}^2 (X^{\mathrm{T}}X)^{-1},\ \hat{\lambda}^2 = \frac{\mathrm{SS_E}}{n-2} \tag{14}$$

The $(1 - \alpha)$% confidence interval of the estimated coefficients is

$$\mathrm{CI} = \pm t_{\alpha/2,n-2}\sqrt{\mathrm{Var}(\beta)} \tag{15}$$

Once estimates of B_3 and C_3 have been obtained for the grouped data, we propose models for them as functions of the mass ratio R in step C. This is done by visual inspection of the trends in plots of estimated B_3 and C_3 with R.

Next, in step D, we obtain estimates of the parameters in the models for B_3 and C_3 by fitting the predictions of B_3 and C_3 using the models to the *grouped* data.

Finally, in step E, we use the estimates of the model parameters obtained in step D to fit the models to the original *ungrouped* data to obtain the final best fit values of the model parameters. The estimates and goodness of fit using each of the models are evaluated to decide the model that best represents the data.

MODEL DETAILS, RESULTS, AND DISCUSSION

In step B, using the methods described above, B_3 and C_3 calculated for each group were plotted against the mass ratio, R,

Table 4. Performance of Model 7

	HES 40 000	HES 200 000	HES 450 000
sum of squared errors, $\mathrm{SS_E}$ (Osm/kg)^2	4.945	1.640	3.788
standard error, SE (Osm/kg)	0.2780	0.1613	0.2414

along with their 95% confidence intervals, as shown in Figures 2 and 3 for HES 200 000 as an example. On the basis of the nature of the plots, four models were considered for B_3 and two for C_3 in step C. For B_3, the possibilities considered were a constant value, a linear relationship between B_3 and R, B_3 as a

dx.doi.org/10.1021/jp403377b | J. Phys. Chem. B 2013, 117, 10231−10240

Table 5. Final Parameters for Model 7*

HES	40 000	200 000	450 000
a	-4.900×10^{1}	-9.493×10^{1}	-3.107×10^{2}
b	2.222×10^{1}	3.191×10^{1}	1.168×10^{2}
c	6.555×10^{-1}	8.201×10^{-1}	7.685×10^{-1}
d	-3.474×10^{5}	-1.107×10^{7}	-2.159×10^{8}

*These values give B in units of molal^{-1} and C in units of molal^{-2}.

power law function of R, and an exponential relationship between B_3 and R. For C_3, the possibilities include zero and a constant value. In addition, a model with B_3 and C_3 both being zero is considered, leading to the nine possible models listed in Table 3. Then, in step D, the initial guesses for the coefficients in the models (a, b, c, and d in Table 3) were obtained by fitting the model predictions to the coefficients estimated from the grouped data. Finally, in step E, the initial guesses obtained in step D were utilized to fit eq 8, with model expressions for B_3 and C_3, to the original ungrouped experimental osmolalities to find the final best fit values of the parameters for each model. Because many of the models for B_3 and C_3 are nonlinear, the MATLAB nonlinear fitting function *fsolve* was used to obtain the best fits, and the target was to minimize the sum of squared errors (SS_E) over the entire data set. Plots of predicted versus

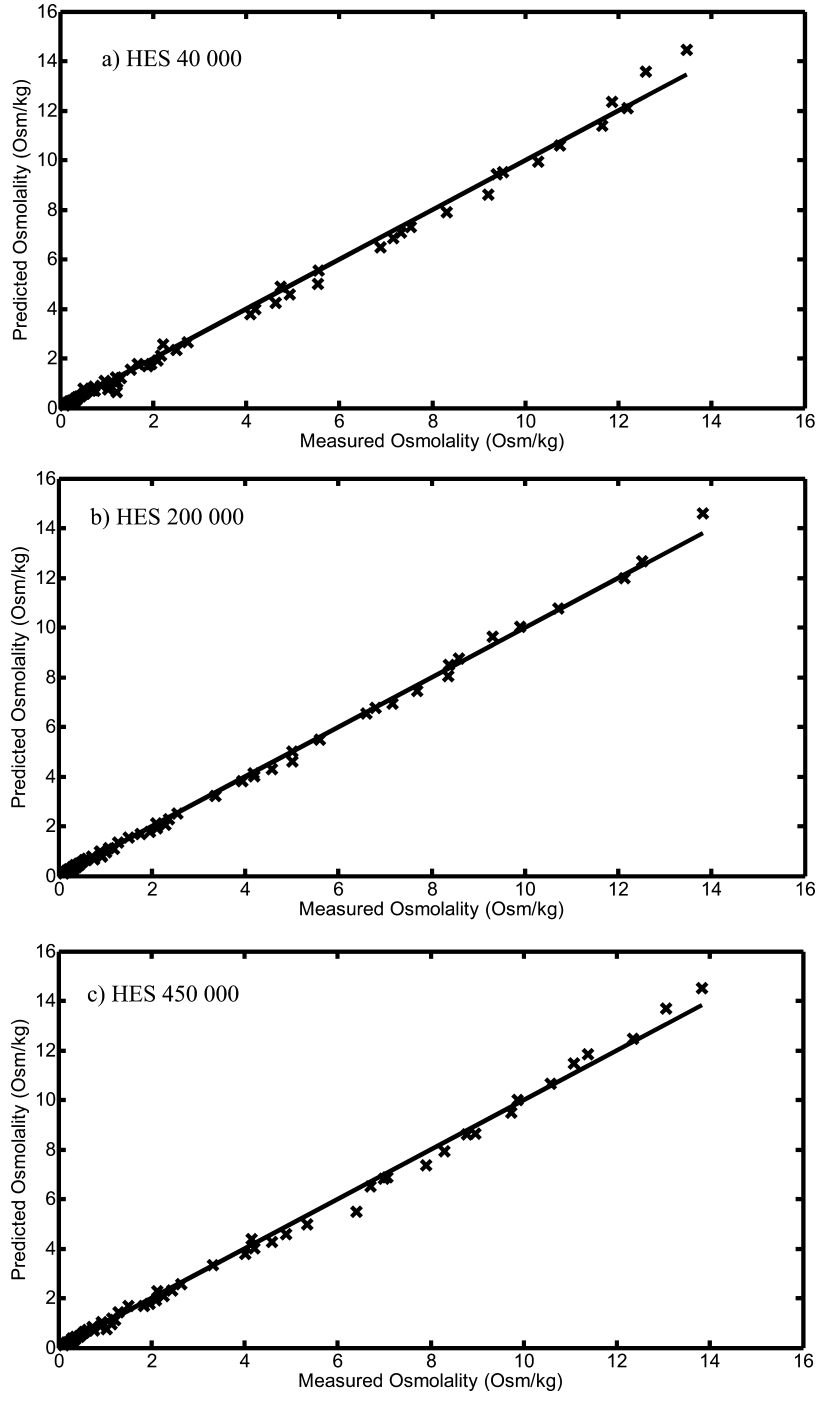

Figure 4. Plots of predicted versus measured osmolality for (a) HES 40 000, (b) HES 200 000, and (c) HES 450 000.

dx.doi.org/10.1021/jp403377b | J. Phys. Chem. B 2013, 117, 10231−10240

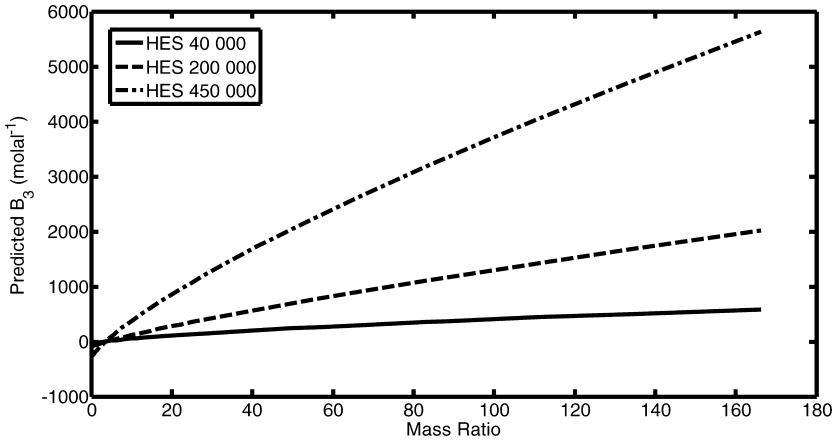

Figure 5. B_3 obtained in this study (i.e., predicted from model 7) as a function of the mass ratio of HES to NaCl for HES 40 000, HES 200 000, and HES 450 000.

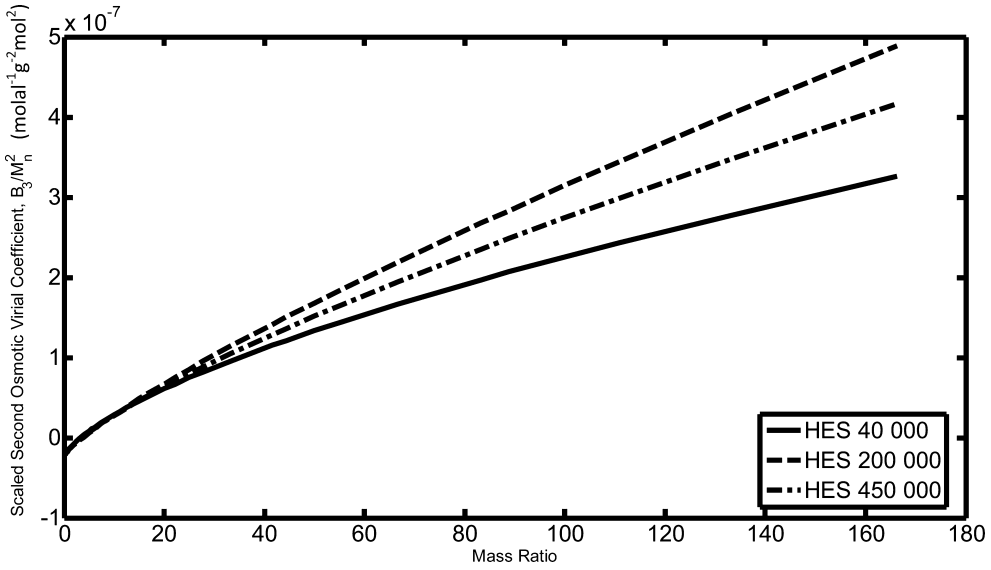

Figure 6. Obtained B_3 from Figure 5 for HES 40 000, HES 200 000, and HES 450 000, scaled with M_n^2 and again plotted as a function of the mass ratio of HES to NaCl.

measured osmolalities for each model are provided for HES 40 000, HES 200 000, and HES 450 000 in the Supporting Information. Though most of the models provided reasonable fits, model 7 consistently had the smallest SS_E and standard error (SE) for all three data sets. Model 7 is of the form

$$B_3 = a + bR^c \tag{16}$$

$$C_3 = d \tag{17}$$

Table 4 shows the sum of squared errors and the standard error with model 7 for each data set, which were found to be 4.945, 1.640, and 3.788 Osm^2/kg^2 (SS_E) and 0.2780, 0.1613, and 0.2414 Osm/kg (SE) for HES 40 000, HES 200 000, and HES 450 000, respectively. Table 5 shows the final estimates of the parameters (a, b, c, and d) used in model 7.

Thus, the final version of the equation that can be used to predict the osmolality of the HES−NaCl−water solution is

$$\pi = k_{diss}m_2 + m_3 + B_2(k_{diss}m_2)^2 + (\boldsymbol{a + bR^c})m_3^2 + (B_2 + (\boldsymbol{a + bR^c}))k_{diss}m_2m_3 + \boldsymbol{d}m_3^3 \tag{18}$$

Figure 4 shows plots of predicted versus measured osmolality using model 7 for the ungrouped data. (The panels of Figure 4 are redrawn on log scales in the Supporting Information.) For all three HES modifications, the predicted osmolality from model 7 was very accurate. Also, no systematic trend was observed in the errors between the predicted and measured osmolalities, which implies that only random errors were not captured in the model. The predicted-versus-measured plots support the conclusion that eq 18, which incorporates model 7, is the best candidate to fit and predict osmolality for HES 40 000, HES 200 000, and HES 450 000 in the range of HES-to-NaCl mass ratios from 0.2 to 166.3.

The second osmotic virial coefficient of large molecules in aqueous salt solutions has been studied before.[38] In Figure 5, the second osmotic virial coefficients found in this study are plotted versus the HES-to-NaCl mass ratio R. A major contributor to the dependence of the second osmotic virial equation on salt concentration is the role of changing double-layer repulsion. As the salt concentration increases (or as R is decreased), the double-layer thickness (also called the Debye screening length) decreases and the double-layer repulsion energy decreases, leading to a decrease in the interaction energy

dx.doi.org/10.1021/jp403377b | J. Phys. Chem. B 2013, 117, 10231−10240

and a decrease in B. Lima et al.[38] modeled the second osmotic virial coefficient of lysozyme in various salt solutions, including double-layer repulsion, van der Waals attraction, and hard sphere repulsion effects, and predicted a decrease in B with salt concentration that is qualitatively similar to that found in Figure 5 (i.e., an increase in B with R).

To compare the influence of individual molecule preparation on solute−solute interactions in solution, the second osmotic virial coefficients can be divided by M_n^2, giving a measure of interaction energy per average repeating unit of the macromolecules and putting the different molecular weight preparations on a comparable basis. Figure 6 shows the second osmotic virial coefficients scaled this way. All three HES preparations show similar interactions per repeating unit at low R, but differences still remain at high R. These differences cannot be simply explained by the degree of substitution, DS, because the DS values for the two lower-molecular-weight HES preparations are the same.

CONCLUSIONS

In this work, we report new aqueous hydroxyethyl starch−sodium chloride (HES−NaCl) vapor pressure osmometry data and have shown that the multisolute osmotic virial equation with appropriate mixing rules can accurately describe the osmolality of three different HES−NaCl solutions. We have also shown that the dependence of the osmotic virial coefficients on the HES-to-NaCl mass ratio for each of these mixtures can be captured using only four fitted parameters. The osmotic virial coefficients at any mass ratio of HES to NaCl can be found by substituting the value of parameters a, b, c, and d from Table 5 into eqs 16 and 17. Thus, solution osmolalities for each HES preparation can be accurately predicted from molalities of HES (m_3) and NaCl (m_2) by substituting the molalities, the mass ratio of HES to NaCl (R), and the value of parameters a, b, c, and d from Table 5 into eq 18. Osmolality is the concentration dependence of the water chemical potential in an aqueous solution and so governs transport in a number of applications including water transport across cell membranes in cryobiology where HES may be used as a cryoprotectant in the presence of NaCl.

In addition to presenting a new extensive data set for osmometry of aqueous solutions of HES and NaCl, the results of this work demonstrate the power of the multisolute osmotic virial approach in describing complex data sets. As well, the understanding gained from these results can give insights into how the osmolality of other HES−NaCl solutions with different HES modifications and molecular weights might be expected to behave.

ASSOCIATED CONTENT

Supporting Information

Plots of predicted versus measured osmolality for all nine models and log-scale versions of Figure 4. This material is available free of charge via the Internet at http://pubs.acs.org.

AUTHOR INFORMATION

Corresponding Author

*Department of Chemical and Materials Engineering, University of Alberta, Edmonton, Alberta T6G 2V4, Canada. Phone: +1 (780) 492-7963. Fax: +1 (780) 492-2881. E-mail: janet.elliott@ualberta.ca.

Notes

The authors declare no competing financial interest.

ACKNOWLEDGMENTS

This research was funded by a Dean's Research Award for J.C. from the Faculty of Engineering, University of Alberta, the Canadian Institutes of Health Research (CIHR MOP 86492, 85068, CPG 75237), and the Natural Sciences and Engineering Research Council (NSERC) of Canada. J.A.W.E. holds a Canada Research Chair in Thermodynamics. A description of the experimental methods and the data in Table 2 appeared in the thesis of Martin Gier.[39]

REFERENCES

(1) Sputtek, A.; Körber, C. Cryopreservation of Red Blood Cells, Platelets, Lymphocytes, and Stem Cells. In *Clinical Applications of Cryobiology*; Fuller, B. J., Gout, B. W. W., Eds.; CRC Press: Boca Raton, FL, 1991.

(2) Sputtek, A.; Kühnl, P.; Rowe, A. W. Cryopreservation of Erythrocytes, Thrombocytes, and Lymphocytes. *Transfusion Medicine and Hemotherapy.* **2007**, *34* (4), 262−267.

(3) Horn, E. P.; Sputtek, A.; Standl, T.; Rudolf, B.; Kühnl, P.; am Esch, J. S. Transfusion of Autologous, Hydroxyethyl Starch-Cryopreserved Red Blood Cells. *Anesth. Analg.* **1997**, *85* (4), 739−745.

(4) Sputtek, A.; Singbartl, G.; Langer, R.; Schleinzer, W.; Henrich, H. A.; Kühnl, P. Cryopreservation of Red Blood Cells with the Non-penetrating Cryoprotectant Hydroxyethyl Starch. *CryoLetters* **1995**, *16*, 283−288.

(5) McMillan, W. G.; Mayer, J. E. The Statistical Thermodynamics of Multicomponent Systems. *J. Chem. Phys.* **1945**, *13* (7), 276−305.

(6) Vilker, V. L.; Colton, C. K.; Smith, K. A. The Osmotic Pressure of Concentrated Protein Solutions: Effect of Concentration and pH in Saline Solutions of Bovine Serum Albumin. *J. Colloid Interface Sci.* **1981**, *79* (2), 548−566.

(7) Haynes, C. A.; Beynon, R. A.; King, R. S.; Blanch, H. W.; Prausnitz, J. M. Thermodynamic Properties of Aqueous Polymer Solutions: Poly(ethylene glycol)/Dextran. *J. Phys. Chem.* **1989**, *93* (14), 5612−5617.

(8) Rathbone, S. J.; Haynes, C. A.; Blanch, H. W.; Prausnitz, J. M. Thermodynamic Properties of Dilute Aqueous Polymer Solutions from Low-Angle Laser-Light-Scattering Measurements. *Macromolecules* **1990**, *23* (17), 3944−3947.

(9) Gaube, J.; Stumpf, M.; Pfennig, A. Thermodynamics of Aqueous Poly(ethylene glycol)-dextran 2-Phase Systems Using the Consistent Osmotic Virial Equation. *Fluid Phase Equilib.* **1993**, *83*, 365−373.

(10) Hasse, H.; Kany, H. P.; Tintinger, R.; Maurer, G. Osmotic Virial Coefficients of Aqueous Poly(ethylene glycol) from Laser-Light Scattering and Isopiestic Measurements. *Macromolecules* **1995**, *28* (10), 3540−3552.

(11) Dobert, F.; Pfennig, A.; Stumpf, M. Derivation of the Consistent Osmotic Virial Equation and Its Application to Aqueous Poly(ethylene glycol)-Dextran Two-Phase Systems. *Macromolecules* **1995**, *28* (23), 7860−7868.

(12) Kany, H. P.; Hasse, H.; Maurer, G. Thermodynamic Properties of Aqueous Poly(vinylpyrrolidone) Solutions from Laser-Light-Scattering, Membrane Osmometry, and Isopiestic Measurements. *J. Chem. Eng. Data* **2003**, *48* (3), 689−698.

(13) Weng, L. D.; Li, W. Z.; Zuo, J. G. DSC Determination of Partial Ternary Phase Diagrams of Methanol/Sodium Chloride/Water and Propylene Glycol/Sodium Chloride/Water and Their Applications for Synthesized Diagrams. *Thermochim. Acta* **2011**, *512* (1−2), 225−232.

(14) Elliott, J. A. W.; Prickett, R. C.; Elmoazzen, H. Y.; Porter, K. R.; McGann, L. E. A Multi-solute Osmotic Virial Equation for Solutions of Interest in Biology. *J. Phys. Chem. B* **2007**, *111* (7), 1775−1785.

(15) Edmond, E.; Ogston, A. G. An Approach to Study of Phase Separation in Ternary Aqueous Systems. *Biochem. J.* **1968**, *109* (4), 569−576.

(16) King, R. S.; Blanch, H. W.; Prausnitz, J. M. Molecular Thermodynamics of Aqueous 2-Phase Systems for Bioseparations. *AIChE J.* **1988**, *34* (10), 1585−1594.
(17) Cabezas, H.; Evans, J. D.; Szlag, D. C. A Statistical Mechanical Model of Aqueous 2-Phase Systems. *Fluid Phase Equilib.* **1989**, *53*, 453−462.
(18) Haynes, C. A.; Blanch, H. W.; Prausnitz, J. M. Separation of Protein Mixtures by Extraction: Thermodynamic Properties of Aqueous 2-Phase Polymer Systems Containing Salts and Proteins. *Fluid Phase Equilib.* **1989**, *53*, 463−474.
(19) Mishima, K.; Nakatani, K.; Nomiyama, T.; Matsuyama, K.; Nagatani, M.; Nishikawa, H. Liquid−Liquid Equilibria of Aqueous 2-Phase Systems Containing Polyethylene Glycol and Dipotassium Hydrogenphosphate. *Fluid Phase Equilib.* **1995**, *107* (2), 269−276.
(20) Li, M.; Zhu, Z. Q.; Wu, Y. T.; Lin, D. Q. Measurement of Phase Diagrams for New Aqueous Two-Phase Systems and Prediction by a Generalized Multicomponent Osmotic Virial Equation. *Chem. Eng. Sci.* **1998**, *53* (15), 2755−2767.
(21) Zafarani-Moattar, M. T.; Gasemi, J. Liquid−Liquid Equilibria of Aqueous Two-Phase Systems Containing Polyethylene Glycol and Ammonium Dihydrogen Phosphate or Diammonium Hydrogen Phosphate. Experiment and Correlation. *Fluid Phase Equilib.* **2002**, *198* (2), 281−291.
(22) Zafarani-Moattar, M. T.; Sadeghi, R. Liquid−Liquid Equilibria of Aqueous Two-Phase Systems Containing Polyethylene Glycol and Sodium Dihydrogen Phosphate or Disodium Hydrogen Phosphate: Experiment and Correlation. *Fluid Phase Equilib.* **2001**, *181* (1−2), 95−112.
(23) Zafarani-Moattar, M. T.; Sadeghi, R.; Hamidi, A. A. Liquid−Liquid Equilibria of an Aqueous Two-Phase System Containing Polyethylene Glycol and Sodium Citrate: Experiment and Correlation. *Fluid Phase Equilib.* **2004**, *219* (2), 149−155.
(24) Prickett, R. C.; Elliott, J. A. W.; Hakda, S.; McGann, L. E. A Non-ideal Replacement for the Boyle van't Hoff Equation. *Cryobiology* **2008**, *57* (2), 130−136.
(25) Elmoazzen, H. Y.; Elliott, J. A. W.; McGann, L. E. Osmotic Transport across Cell Membranes in Nondilute Solutions: A New Nondilute Solute Transport Equation. *Biophys. J.* **2009**, *96* (7), 2559−2571.
(26) Abazari, A.; Elliott, J. A. W.; Law, G. K.; McGann, L. E.; Johma, N. M. A Biomechanical Triphasic Approach to the Transport of Nondilute Solutions in Articular Cartilage. *Biophys. J.* **2009**, *97* (12), 3054−3064.
(27) Ross-Rodriguez, L. U.; Elliott, J. A. W.; McGann, L. E. Investigating Cryoinjury Using Simulations and Experiments: 1. TF-1 Cells during Two-Step Freezing (Rapid Cooling Interrupted with a Hold Time). *Cryobiology* **2010**, *61* (1), 38−45.
(28) Ross-Rodriguez, L. U.; Elliott, J. A. W.; McGann, L. E. Investigating Cryoinjury Using Simulations and Experiments: 2. TF-1 Cells Graded Freezing (Interrupted Slow Cooling without Hold Time). *Cryobiology* **2010**, *61* (1), 46−51.
(29) Benson, J. D.; Bagchi, A.; Han, X.; Critser, J. K.; Woods, E. J. Melting Point Equations for the Ternary System Water/Sodium chloride/Ethylene glycol Revisited. *Cryobiology* **2010**, *61* (3), 352−356.
(30) Han, X.; Liu, Y.; Critser, J. K. Determination of the Quaternary Phase Diagram of the Water-Ethylene Glycol-Sucrose-NaCl System and a Comparison between Two Theoretical Methods for Synthetic Phase diagrams. *Cryobiology* **2010**, *61* (1), 52−57.
(31) MacNeil, J. A.; Ray, G. B.; Leaist, D. G. Activity Coefficients and Free Energies of Nonionic Mixed Surfactant Solutions from Vapor-Pressure and Freezing-Point Osmometry. *J. Phys. Chem. B.* **2011**, *115* (19), 5947−5957.
(32) Abazari, A.; Thompson, R. B.; Elliott, J. A. W.; McGann, L. E. Transport Phenomena in Articular Cartilage Cryopreservation As Predicted by the Modified Triphasic Model and the Effect of Natural Inhomogeneities. *Biophys. J.* **2012**, *102* (6), 1284−1293.
(33) Prickett, R. C.; Elliott, J. A. W.; McGann, L. E. Application of the Osmotic Virial Equation in Cryobiology. *Cryobiology* **2010**, *60* (1), 30−42.
(34) Prickett, R. C.; Elliott, J. A. W.; McGann, L. E. Application of the Multisolute Osmotic Virial Equation to Solutions Containing Electrolytes. *J. Phys. Chem. B.* **2011**, *115* (49), 14531−14543.
(35) Jochem, M.; Körber, C. Extended Phase-Diagrams for the Ternary Solutions H_2O-NaCl-Glycerol and H_2O-NaCl-Hydroxyethyl-starch (HES) Determined by DSC. *Cryobiology* **1987**, *24* (6), 513−536.
(36) Prausnitz, J. M.; Lichtenthaler, R. N.; de Azevedo, E. G. *Molecular Thermodynamics of Fluid-Phase Equilibria*, 3rd ed; Prentice Hall: Upper Saddle River, NJ, 1999.
(37) Savitsky, A.; Golay, M. J. E. Smoothing and differentiation of data by simplified least squares procedures. *Anal. Chem.* **1964**, *36* (8), 1627−1639.
(38) Lima, E. R. A.; Biscaia, E. C., Jr.; Boström, M.; Tavares, F. W.; Prausnitz, J. M. Osmotic Second Virial Coefficients and Phase Diagrams for Aqueous Proteins from a Much-Improved Poisson−Boltzmann Equation. *J. Phys. Chem. C.* **2007**, *111*, 16055−16059.
(39) Gier M. Der Einfluß des Kolloids Hydroxyethylstärke (HES) auf den osmotischen Druck wäßriger Elektrolytlösungen. Diploma Thesis. Fachhochschule Aachen, Abteilung Jülich, 1992.